Phase Behavior of I_2S Single Graft Block Copolymer/Homopolymer Blends

Lizhang Yang and Samuel P. Gido*

Polymer Science and Engineering Department, W. M Keck Electron Microscopy Laboratory, University of Massachusetts, Amherst, Massachusetts 01003

Jimmy W. Mays

Department of Chemistry, University of Alabama at Birmingham, Birmingham, Alabama 35294

Stergios Pispas and Nikos Hadjichristidis

Department of Chemistry, University of Athens, Panepistimiopolis Zografou 15771, Athens, Greece

Received November 3, 2000; Revised Manuscript Received February 23, 2001

ABSTRACT: This work is part of an extensive study of model nonlinear block copolymer/homopolymer blends. Effects of graft molecular architecture on the morphology of block copolymer/homopolymer blends have been examined. The single graft Y-shaped block copolymers used in the study are I_2S block copolymers, which have two low polydispersity (PDI) polyisoprene arms and one low PDI polystyrene arm joint at a single junction point. Previously reported linear diblock copolymer/homopolymer blend systems showed that the order−order transitions (OOTs) occur at about the same volume fractions as in pure linear diblock copolymers. The OOT occurs at the same volume fraction regardless of the direction from which it is approached, i.e., blending homopolymer A with a diblock which forms A cylinders in a B matrix to push it toward lamella or blending B homopolymer with a lamellar diblock to push it back toward cylinders. This study shows that when a homopolymer is blended with an I_2S block copolymer, the OOTs split so that they occur at different volume fractions depending up whether they are approached by blending homopolymer into the two-arm or the one-arm side of the block copolymer interface. A perforated lamellar morphology is obtained in a blend of homopolystyrene (hPS) and a lamella forming single graft block copolymer, and it is found to be stable to thermal annealing.

Introduction

Recently, there have been many investigations concerning the effects of graft block copolymer molecular architecture on morphology using well-defined, *model* branched block copolymer materials.[4−12] The present study investigates the effect for molecular asymmetry and graft architecture on blend morphology. The morphologies of neat microphase-separated A_2B single graft copolymers have been studied by Pochan, Gido, et al.[4,5] The results of the experimental study were plotted on a theoretical morphology diagram for asymmetric miktoarm stars, calculated by Milner.[13] For architecturally and conformationally asymmetric miktoarm stars of type A_nB_m, this theory predicts morphology as a function of *B* component volume fraction, ϕ_B, and a molecular asymmetry parameter, $\epsilon = (n_A/n_B)(l_A/l_B)^{1/2}$. Here, n_A and n_B are the numbers of arms of block materials A and B, and $l_i = (V_i/R_i^2) = v_i/b_i^2$. V_i and R_i are volume and radius of gyration of one arm of polymer *i*, while v_i is the segmental volume and b_i the statistical segment length of component *i*. The morphologies observed for the A_2B materials showed general agreement with the shift in composition ranges predicted by the theory. However, for some samples, the Milner calculation slightly overestimated the degree of shift in the order−order transitions.[4] Some other studies on S_2I, I_2S, and I_3S also showed qualitative agreement but quantitative disagreement.[10−12,14−16] The Milner diagram is calculated for pure block copolymer. In this study, we will try to use it as a guide to understand the effects of homopolymer blending on the morphological transitions of I_2S block copolymer systems.

Linear diblock copolymer/homopolymer blends and linear multiblock copolymer/homopolymer blends systems have been extensively studied.[1−3,17−26] Previously reported linear diblock copolymer/homopolymer blend results showed that the OOTs in the blends occur at about the same volume fractions as those of pure linear diblock copolymers.[1−3] However, for architecturally asymmetric graft copolymers, blending homopolymer into the one arm side or into the multiarm side of the interface may produce different morphological results. In the present study, I_2S block copolymers are blended with homopolymers of polystyrene (hPS) or homopolymer polyisoprene (hPI).

One of the blends in this study is observed to form a hexagonally perforated lamellar structure. Hexagonally perforated lamellae, which resemble the cantenoid−lamellar structure derived by periodic area-minimizing surface calculations,[27] were also observed recently in linear diblock systems,[28−35] in a narrow volume fraction region between HEX and LAM. Several linear block copolymer/homopolymer blends have been previously shown to form perforated lamellar structures.[23,36] To date, however, ordered perforated lamellar structures have not been observed in block copolymers or blends involving block copolymers with graft architectures.

Controversy exists regarding the details of the perforated lamella structure and the stability of the morphology. Both ABC stacking of the hexagonally perforated layers[29,35] and a combination of an ABC and AB stacking[31] were suggested for the perforated

* To whom correspondence should be addressed.

10.1021/ma001901v CCC: $20.00
Published on Web 05/11/2001

Table 1. Molecular Characterization of the I_2S Block Copolymer and the PS and PI Homopolymers

sample name	M_n(PS arm)[a] ($\times 10^{-3}$)	M_n(PI arm)[a] ($\times 10^{-3}$)	M_n(total)[a]	M_w/M_n[b]	wt % d-PS[c]	vol % d-PS[d]	$2\pi/q^*$ ($\pm$0.5 nm)[e]	morphology[e]
I_2S-89	87.3	4.6[e]	97.1×10^3	1.04	91	89		worm
I_2S-81	79.1	9.6	89.4×10^3	1.04	84	81	31.0	cylinder
I_2S-62	61.2	14.8	83.0×10^3	1.04	67	62	39.0	lamella
hPS			870	1.03				
hPI			872	1.17				

[a] Membrane osmometry. [b] SEC. [c] SEC−UV. [d] The vol % was calculated utilizing the density of d-PS = 1.14 g/mL at 25 °C and density of PI = 0.91 g/mL at 25 °C[48] along with the weight percent compositions from SEC−UV. [e] Data from ref 4.

Table 2. Composition and Morphology of the Blends in the Study

sample name	wt fraction of homopolymer	overall wt fraction of PS	[a]overall vol fraction of PS	morphology	$2\pi/q^*$ ($\pm$ 0.5 nm)[b]
IY 89−86	0.032	0.88	0.86	worm	
IY89−82	0.068	0.85	0.82	vesicle and sheet	
IY89−80	0.081	0.83	0.80	disordered layer and vesicle	
IY89−77	0.12	0.80	0.77	disordered layer and vesicle	
IY89−71	0.17	0.75	0.71	disordered layer and vesicle	
IY81−80	0.013	0.83	0.80	cylinder	33.3
IY81−76	0.045	0.80	0.76	cylinder	33.3
IY81−73	0.083	0.77	0.73	cylinder	34.5
IY81−71	0.12	0.75	0.71	cylinder	35.2
IY81−66	0.16	0.71	0.66	cylinder	37.5
IY81−65	0.17	0.70	0.65	lamella	40.4
SY81−82	0.062	0.85	0.82	cylinder	31.6
SY81−85	0.25	0.88	0.85	disordered cylinder	30.6
SY62−73	0.30	0.77	0.73	lamella	38.5
SY62−76	0.39	0.80	0.76	lamella	39.4
SY62−79	0.48	0.83	0.79	lamella	40.0
SY62−82	0.54	0.85	0.82	perforated lamella	37.5
SY62−85	0.64	0.88	0.85	cylinder	35.2
SY62−89	0.72	0.91	0.89	cylinder	36.2

[a] Calculated utilizing density of (d-PS) = 1.14 g/mL at 25 °C and density of PI = 0.91 g/mL at 25 °C.[48] [b] $q^* = 4\pi/\lambda(\sin\theta_1)$ and $2\theta_1$ is the scattering angle for the lowest angle Bragg peak; corresponds to $d_{(100)}$ for hexagonal packed cylinders, $d_{(001)}$ for lamellae, respectively.

lamellar morphology. Using the methods of Semenov[37] to estimate the free energy of perforated lamella in the strong segregation limit (SSL), Fredrickson[38] showed that the perforated lamella is metastable with respect of cylinders and lamella at $\phi = 0.35$. Qi and Wang[39−41] showed that the perforated lamellae appear as a "pseudostable" morphology during the lamellar to cylinder transition.

Experimental Section

The synthesis of the I_2S block copolymers and the subsequent molecular characterization was described in a previous publication.[4] The materials were produced by anionic polymerization under high vacuum in all glass reactors. The graft architecture was generated using coupling with trichloromethylsilane. The volume fraction and morphology of the neat I_2S block copolymers and homopolymers used in this study are listed in Table 1. The polystyrene of both the I_2S block copolymers and the homopolymer were deuterated. We use low molecular weight (MW) homopolymer in all the blend systems so that the distribution of the homopolymer within the block copolymer domains of like material is relatively uniform.[18,21,42] This study utilizes blends which have overall high PS composition. Blends with I_2S block copolymers having high overall PI composition have been examined separately.[43]

Graft copolymer and homopolymer in the proportions to give the desired blend were co-dissolved in toluene, a nonpreferential solvent. Solid films approximately 1 mm thick were slowly cast from these co-solutions at room temperature over the course of 10−14 days. Residual toluene was removed by placing the samples under vacuum at ambient temperature for another week. Each sample was thermally annealed in a vacuum oven at 120 °C for 2 weeks to further promote the approach to equilibrium. The samples were then cooled under vacuum to room temperature over a period of several hours.

Sample morphologies were characterized using a combination of transmission electron microscopy (TEM) and small-angle X-ray scattering (SAXS). To prepare thin sections for microscopy, a Leica Ultracut UCT microtome equipped with a Leica EM FCS cryogenic sample chamber operated at −110 °C was used to cut sections approximately 500 Å in thickness. The sections were collected on TEM grids and stained for 4 h in OsO_4 vapor. The PI microdomains are preferentially stained by OsO_4, rendering them dark relative to PS microdomains due to mass-thickness contrast in the TEM. A JEOL 100CX TEM, operated at an accelerating voltage of 100 kV, was used to image the stained sections. SAXS data were collected at the Advanced Polymers Beamline (X27C), located at the National Synchrotron Light Source at Brookhaven National Labs (BNL), Upton, NY. Two-dimensional scattering patterns were collected on Fujitsu image plates, then read by a Fujitsu BAS 2000 image plate reader. Custom software at BNL was used to subtract background noise and perform circular averaging. Data were collected for a wavelength of 1.307 Å and a camera length of 1410 mm.

Four different series of blends are examined. Blends are designated as either IY$n-m$ or SY$n-m$. The first character, I or S, indicates that the homopolymer used in the blend series is either homopolyisoprene (I) or homopolystyrene (S). The first number n indicates the PS volume fraction of the Y-shaped graft copolymer (I_2S-89, I_2S-81, or I_2S-62 from ref 4) on which the blend series is based. The last number, m, indicates the PS volume fraction of the overall blend after addition of homopolymer. The molecular characteristics of the block copolymers and homopolymers are listed in Table 1. The compositions of all the blends studied in this paper are given in Table 2.

Results

(1) SY62 Series. The pure single graft block copolymer I_2S-62 with polystyrene volume fraction ϕ_{PS} = 62% formed a lamellar morphology with a long period

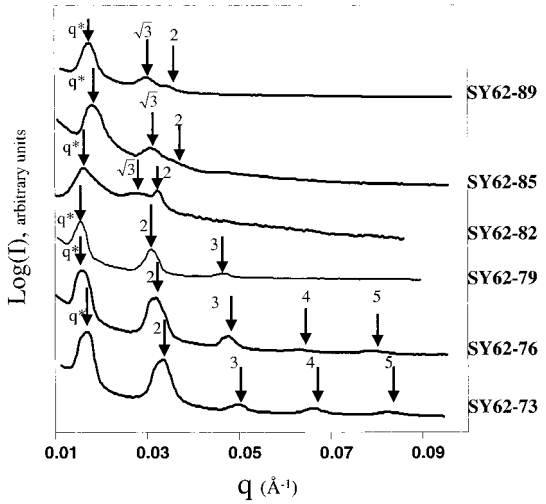

Figure 1. Isotropic SAXS patterns of SY62 series blends azimuthally integrated into one-dimensional plots of log(*I*) vs *q*.

of 39.0 ± 0.5 nm.[4] The SAXS data for the SY62 blend series are shown in Figure 1. The first three blends, SY62−73, SY62−76, and SY62−79, maintain the lamellar morphology with slightly increasing lamellar spacing (Table 2). The fourth blend, SY62−82, forms perforated lamella. The layer spacing of perforated layers is 37.5 nm, which is a decrease from the lamellar spacing of SY62−79 due to the morphology change. The $\sqrt{3}q^*$ reflection results from the ordering of the perforations.[31,35] These scattering data do not permit the determination of detailed structural information about the stacking of the perforated layers. The perforated lamellar morphology persisted upon annealing at 120 °C for 2 weeks. Figure 2 shows two TEM images of SY62−82. Shown in Figure 2a, when the microtome direction is parallel to the lamellar layers of the perforated lamellar structure and thus the TEM projection direction is perpendicular to the layers, the projection appears like a hexagonal honeycomb mesh of dark PI perforated by holes of light PS. This image is striking for its illustration of the relatively thin meshlike structure in the PI layer that results from the low PI volume fraction of 0.18 in this blend. The fact that a perforated lamellar structure is found at this unusual composition is a direct result of the I_2S molecular architecture of the block copolymer used in the blend.

Figure 2b illustrates the TEM images obtained when the microtoming cuts perpendicular to the layered structure and thus the TEM projection occurs parallel to the layers. Different images are possible depending upon the direction of projection within the layer of perforations and on the way in which the thin section intersects the three-dimensional structure. A detailed analysis of all the possible projected images of the perforated lamellar structure is beyond the scope of this paper, and some analysis of these projections has been given previously by Bates and co-workers.[29] Figure 2b shows a TEM image corresponding to projection parallel to the layers where the dark spots result from the cross section of parts of the PI mesh structure.

As the PS volume fraction further increases, the blends SY62−85 and SY62−89 both form cylindrical morphologies, and the cylinder (100) *d* spacing increases as the homopolymer volume fraction increases (Table 2). TEM observation (data not shown) confirmed the cylindrical morphologies of SY62−85 and SY62−89. The

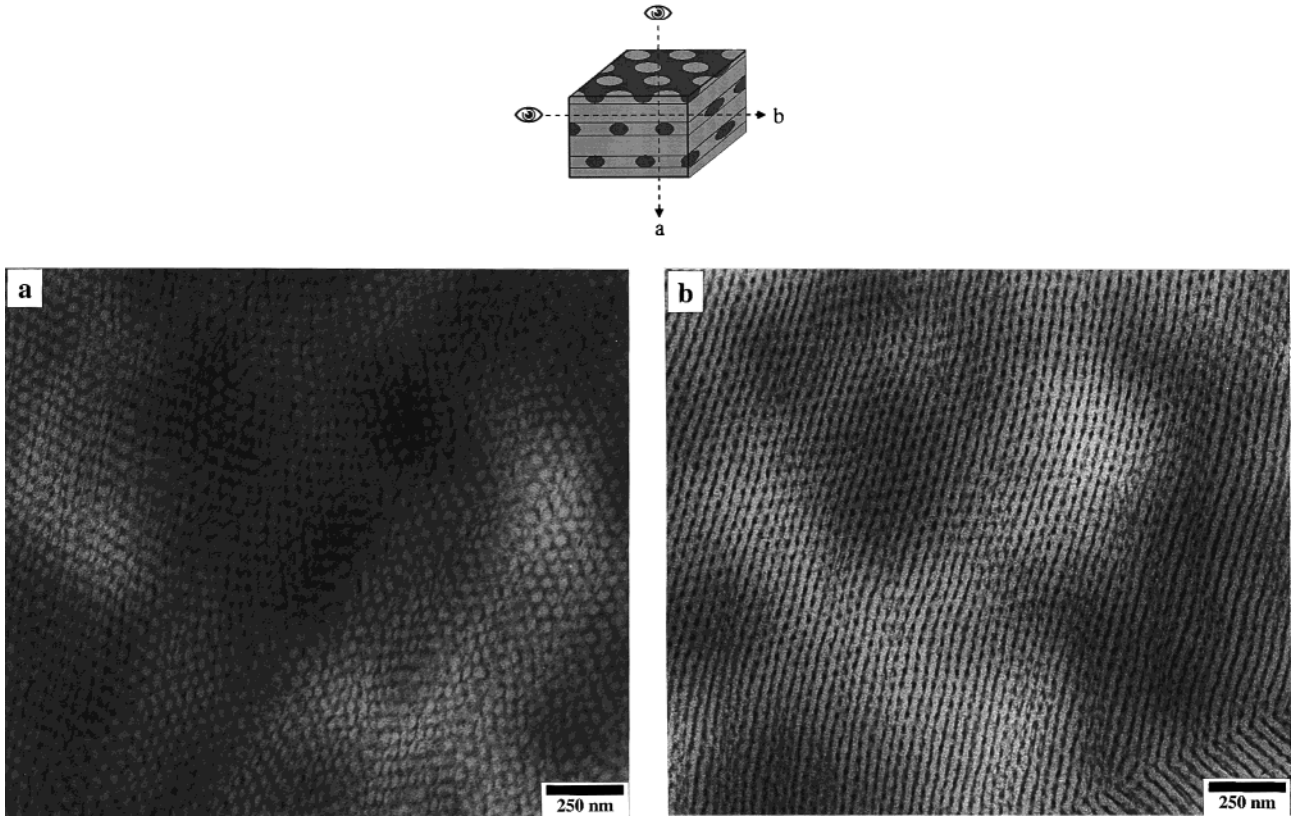

Figure 2. TEM images of blend SY62−82. (a) TEM projection direction is seen perpendicular to the layers of the perforated lamellar structure. The TEM image appears like a hexagonal honeycomb mesh of dark PI perforated by holes of light PS. (b) When the TEM projection is parallel to the layers, the rows of dark spots result from the cross section of parts of the PI mesh structure.

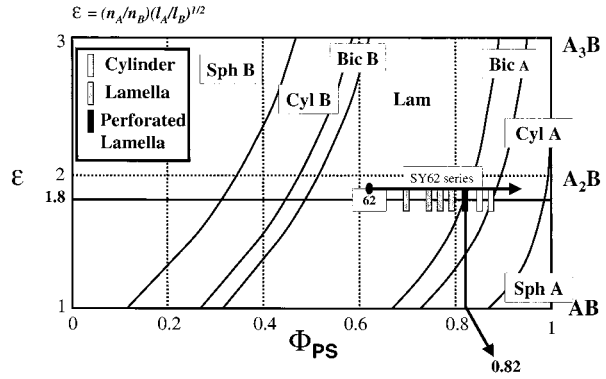

Figure 3. SY62 blend series mapped onto the theoretical morphology diagram. The "62" symbol along the solid line at $\epsilon = 1.8$ indicates the volume fraction of the pure I_2S-62 sample upon which the blends are based. The small rectangular boxes indicate the volume fraction of each blend in the series. The shading of the boxes indicates the morphology.

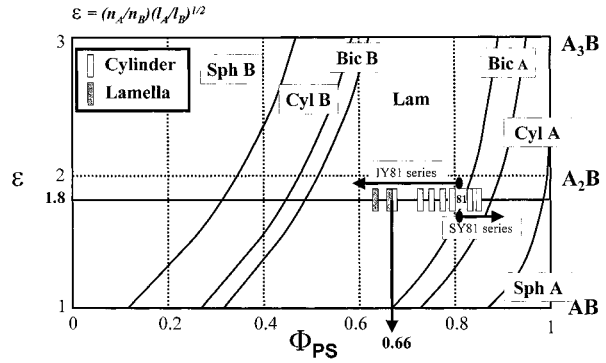

Figure 4. SY81 and IY81 blend series mapped onto the theoretical morphology diagram. The "81" symbol along the solid line at $\epsilon = 1.8$ indicates the volume fraction of the pure I_2S-81 sample upon which the blends are based. The small rectangular boxes indicate the volume fractions of each blend. The shading of the boxes indicates the morphology.

morphologies of the SY62 blends series are mapped onto the theoretical morphology diagram in Figure 3.

SY81 Series. The pure single graft block copolymer I_2S-81 with polystyrene volume fraction $\phi_{PS} = 81\%$ formed a regular cylinder morphology with reported cylinder 100 spacing of 31.0 ± 0.5 nm.[4] The two blend samples of the SY81 series were made by blending low molecular weight homopolystyrene with I_2S-81. The morphologies of the SY81 blend series are mapped onto the morphology diagram in Figure 4. TEM images of SY81−82 and SY81−85 are shown in Figure 5. The long-range order of the morphology decreases as hPS concentration increases and essentially vanishes for SY81−85. The SAXS data shown in Figure 6 support this conclusion. The (100) spacings of SY81−82 and SY81−85, 31.6 and 30.6 nm respectively, are nearly the as same as that of pure I_2S-81. The secondary peak of SY81−85 is broad and weak. We calculated form factor scattering that results from disordered arrangements of domains of spheres and cylinders. Domain sizes are obtained by using the primary peak to get an average center-to-center distance between neighboring domains. This spacing along with the known PS and PI volume fraction can be used to calculate sphere and cylinder radii provided that a model for how the domains fill space is assumed. For the purposes of these calculations cylinder radii were obtained assuming a hexagonal packing and sphere radii were determined using both bcc and SC lattice packings.[44,45] All the form factors for cylinders and spheres (both bcc and SC) fit the data poorly. This suggests that the broad peak is actually from weak and diffuse $\sqrt{3}q^*$ and $2q^*$ Bragg reflections, and the sample has a poorly ordered cylindrical morphology. Both TEM and SAXS indicate that the long-range order of the cylinder morphology decreases as more PS homopolymer is added.

IY81 Series. The morphologies of the IY81 blend series are also mapped onto the morphology diagram in Figure 4. In this series, in which hPI is blended into I_2S-81, samples IY81−80, IY81−76, IY81−73, IY81−71, and IY81−66 all form cylindrical morphologies. Figure 7a shows a TEM image of one of these cylindrical morphologies (IY81−66); the others are similar. There is little change in long-range order with increasing hPI concentration among these cylindrical samples but all are quite well ordered as compared to the SY81 series. With only 1 vol % more PI, blend IY81−65 changed to the lamellar morphology. No intermediate morphology, such as gyroid or perforated lamella, was observed between lamellae and cylinders in this series. Figure 8 shows the SAXS data for this series. The cylinder (100) spacings, shown in Table 2, increased with increasing amounts of homopolyisoprene in the blends.

IY89 Series. The pure single graft block copolymer I_2S-89, with $\phi_{PS} = 0.89$, formed a morphology of disordered, wormlike cylinder domains of PI in a matrix of PS.[4,5] TEM images of the IY89 series, which are produced by blending increasing amounts of hPI with I_2S-89, are shown in Figure 9. Figure 9a reveals that IY89−86 formed a disordered wormlike cylinder morphology, similar to pure I_2S-89. Figure 9b is a TEM image of blend IY89−82 showing that the dark stained PI domains form ringlike structures and short line segments. Figure 10 shows a higher magnification TEM tilt series that reveals that some PI domains which appear as short line segments, are actually pieces of sheets. Some PI domains which appear as rings are actually sections through vesicles, and other objects seem to be caps sectioned off the top or bottom of vesicles. The thickness of these PI sheets is about 12 nm. The diameters of the vesicles as well as the lengths of the PI sheets are about 150−500 nm. The morphology of IY89−82 is composed of bilayer sheets which tend to form closed vesicles or isolated sheets which seem to be limited in their lateral extent to an upper limit of about 40 times the PI layer thickness. Blends IY89−80, IY89−77, and IY89−71 with increasing PI volume fractions also formed sheetlike morphologies but in these cases closed vesicles were not favored (although a few isolated vesicles can be observed in the TEM images). The predominant structures were continuous, convoluted sheets which extend over great distances relative to their sheet thickness. A TEM image of this structure in IY89−80 is shown in Figure 9c. Because of the lack of lattice order in the IY89 blend series, SAXS data were not used for structural investigation. The vesicle and sheet structures of the IY89 series are unusual because the spaces inside the vesicles and between vesicles and/or sheets are frequently much larger (up to almost 1 μm in size) than the radii of gyration of the PS blocks of the I_2S-89 block copolymer (PS molecular weight of 87 300). The TEM images suggest that the vesicles and sheets grow by formation of organized block copolymer bilayers in a matrix of un-microphase-separated material.

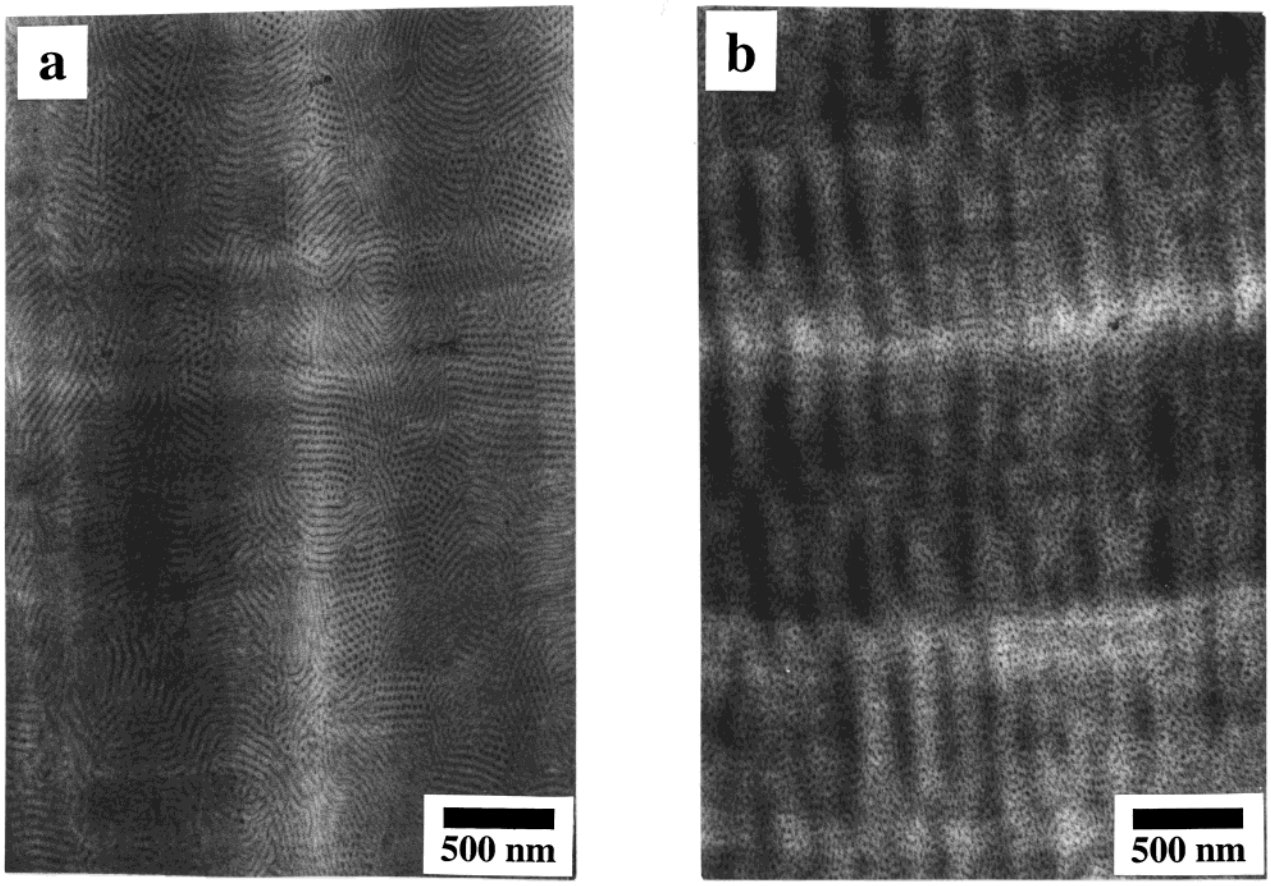

Figure 5. TEM micrographs of blends in the SY81 series: (a) SY81−82 showing projections both parallel and perpendicular to the PI cylinders; (b) SY81−85 showing microphase-separated but not well-ordered morphology.

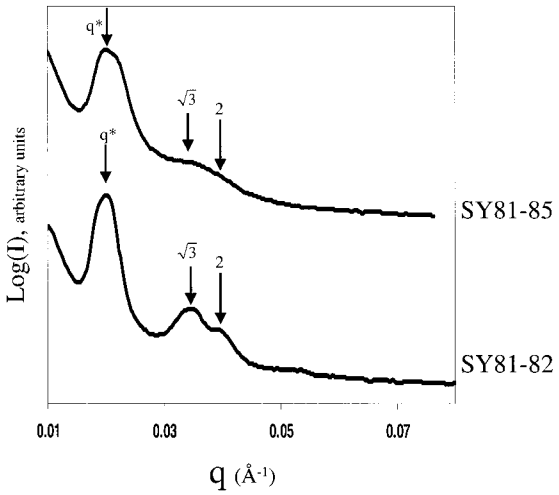

Figure 6. Isotropic SAXS patterns of SY81 series samples azimuthally integrated to give plots of log(*I*) vs *q*.

Discussion

For the lamella samples in the SY62 series, the polystyrene brush height and the polyisoprene brush height can be calculated by $h_{PS} = (1/2)d_{lam}*\phi_{PS}$ and $h_{PI} = (1/2)d_{lam}*\phi_{PS}$, respectively, where d_{lam} is the long period of the lamella structure. The area per block copolymer chain junction can be calculated by $A = M_{PI}/(d_{lam}*\phi_{PI}*\rho_{PI}*N_{av})$, where M_{PI} is the average total molecular weight of the two PI arms of each block copolymer molecule, ρ_{PI} is the density of polyisoprene, and N_{av} is Avogadro's number. After blending in homopolymer, the PS domains swell both parallel and perpendicular to the interface. We can calculate the relative vertical expansion of the PS domain in the blends with respect to the PS brush height of the pure block copolymer (I_2S-62): $\lambda^{\perp} = h/h_o$ where h_o is the PS brush height of the pure block copolymer I_2S-62, and h is the PS brush height of the blend sample. From the area per junction of each blend, the relative expansion ratio in the direction parallel to the interface is calculated by $\lambda'' = (A/A_o)^{0.5}$. Therefore, the total swelling of the PS domains can by expressed by the two expansion ratios: $V/V_o = \lambda^{\perp}(\lambda'')^2$. If the domain expansion is uniform in all directions, $V/V_o = \lambda^3$, with $\lambda = \lambda^{\perp} = \lambda''$; if the expansion is anisotropic then $\lambda^{\perp}$ and λ'' will not be equal and we define their ratio as the expansion asymmetry coefficient: $K = \lambda^{\perp}/\lambda''$. All the calculated results are listed in Table 3 and the asymmetry coefficient for lamella forming SY62 series blends vs homopolymer volume fraction is plotted in Figure 11, from which it is apparent that $K \approx 1$ and changes little with increasing hPS concentration.

The cylinder core radii R of the samples in the IY81 and SY81 blend series were calculated from the (100) interplanar spacing determined by SAXS and the volume fraction of PI ($R_{cyl} = d_{hex(100)}([\phi_{PI}/\pi] \sin [\pi/3])^{1/2}$). The area per block copolymer chain junction can be calculated by $A = (2M_{PI}/(\rho_{PI}R_{cyl}N_{av})$. For the IY81 series, M_{PI} is the effective total polyisoprene molecular weight per junction point which includes the PI content of a single block copolymer molecule as well as the total amount of hPI per block copolymer molecule. This is calculated by dividing the total number of hPI molecules in the system by the total number of block copolymer molecules. We use the cylinder core radius R_{cyl} as the

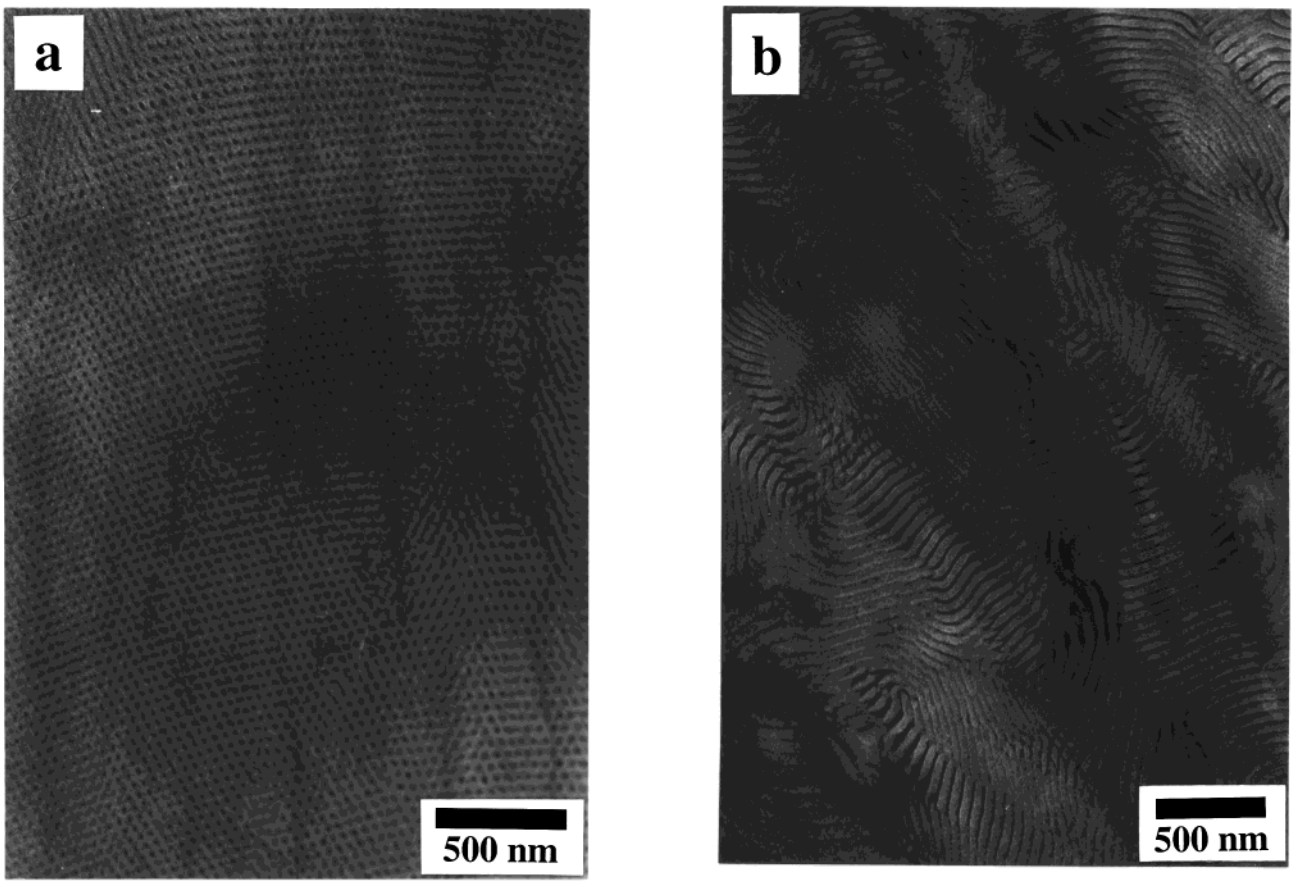

Figure 7. TEM micrographs from the IY81 series: (a) IY81−66 showing a projection perpendicular to PI cylinders; (b) IY81−65 showing a lamellar structure.

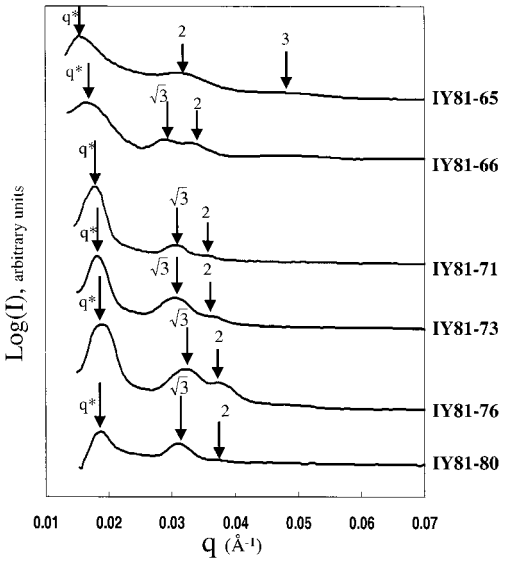

Figure 8. Isotropic SAXS patterns of IY81 series samples azimuthally integrated to give plots of log(*I*) vs *q*.

average PI brush height; the polystyrene brush height can be calculated by $h_{PS} = (\sqrt{3}\ d_{hex(100)}{}^2/\pi)^{1/2} - R_{cyl}$. From these values, λ'', $\lambda^{\perp}$, and K are calculated for the IY81 and the SY81 series and are listed in Table 3. The asymmetry swelling coefficient K is plotted vs homopolymer volume fraction in Figure 11 for cylinder forming blends in both the SY81 and the IY81 series.

Figure 11 shows that expansion coefficients K of the SY62 series and the SY81 series are close to one and change little with increasing ϕ_{PS}. Thus, $\lambda^{\perp} \approx \lambda''$; i.e., in both series, the homopolystyrene swells the PS domains homogeneously. Because the PS and PI domains share the same interface, the component of PS domain swelling parallel to the interface in the SY81 series leads, through conservation of volume, to a decrease of the brush height in the PI domains. Consequently, the overall structural periodicity, the sum of the PS and PI domain thicknesses, changes very little (Table 2). This behavior is considerably different from the IY81 series in which swelling perpendicular to the interface is favored. This can be seen in Figure 11 where K increases with increasing hPI content. As hPI is added, the PI layer thickness increases much more strongly than the interfacial area per junction. In this case the overall structural periodicity was found to increase rather strongly with the addition of hPI as indicated in Table 2.

Previously published studies on the swelling behavior of block copolymer/homopolymer blends, indicate that the degree to which homopolymer penetrates into the brush of the corresponding block of the copolymer depends on the ratio, α, of the homopolymer molecular weight to the molecular weight of the block of the same type.[18,21,42,46] In both the SY62 and SY81 series $\alpha = 0.01$, and in the IY81 series $\alpha = 0.09$. Therefore, a comparison of swelling behavior on the two arm PI side of the interface to that on the one arm PS side of the interface is potentially complicated by a difference in α. However, comparison to data of Winey, Thomas, and Fetters[21] on blends of linear diblocks with homopolymer, also plotted in Figure 11, suggest that the molecular architecture effect on I_2S containing blends is significant enough to be distinguishable even with the α difference.

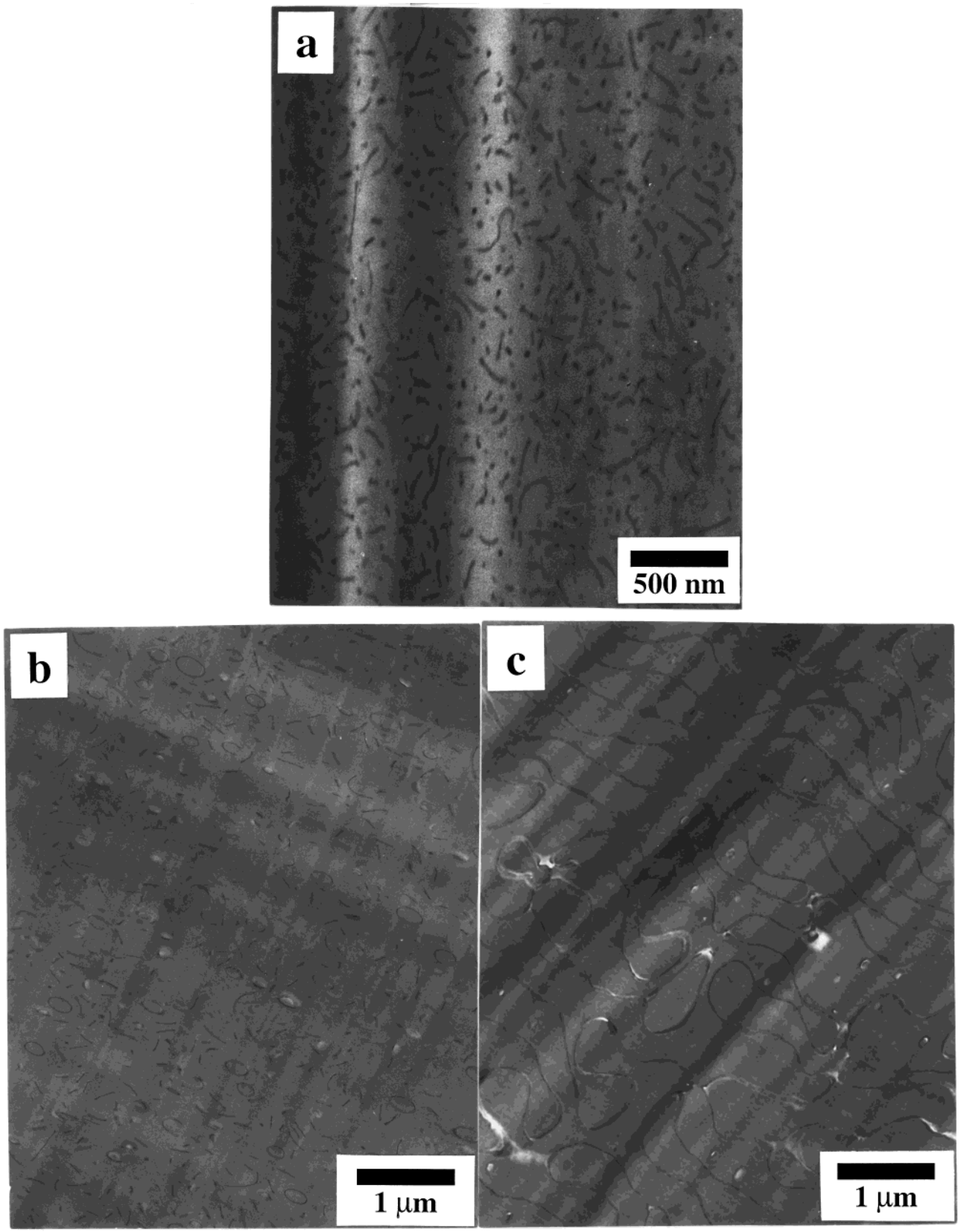

Figure 9. TEM micrographs from the IY89 blend series: (a) IY89−86 showing dark PI wormlike micelles in the PS graft matrix; (b) IY89−82 showing that dark PI domains form ring like structures and short line segments embedded in the PS graft matrix; (c) IY89−80 showing continuous, convoluted PI sheets which extend over great distances relative to their sheet thickness.

The linear diblock swelling data in Figure 11 indicate that with $\alpha = 0.1$, 2600 g/mol hPS swells the PS domain of PS-*b*-PI (PS 27 000 g/mol, PI 22 000 g/mol) relatively homogeneously. The SY62 and SY81 series, with $\alpha = 0.01$, both show similarly isotropic swelling behavior. This observation is consistent with theoretical calculations of Matsen[46] and Shull and Winey[42] which indicate that, at α below 0.125−0.10, homopolymer homogeneously swells the like block of a linear diblock. This suggests that, in the IY81 blend series with $\alpha = 0.09$,

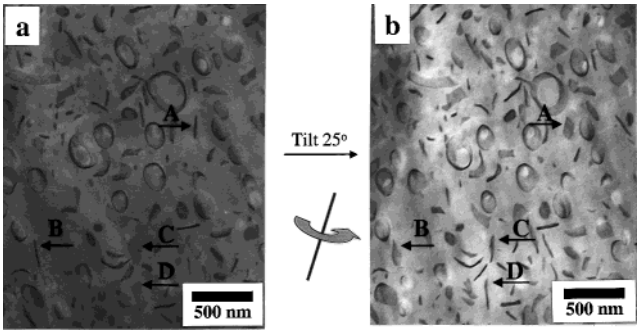

Figure 10. TEM tilt series of IY89−82: (a) 0° tilt; (b) 25° tilt about axis indicated. After tilting, the black PI line segments A and B in part a become PI sheets in part b. The PI sheets C and D in part a become line segments in part b.

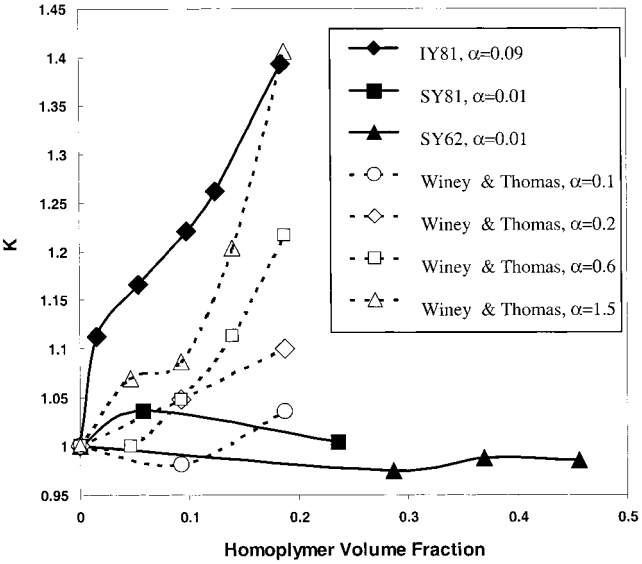

Figure 11. Plot of asymmetry swelling ratio, *K*, vs homopolymer volume fraction for the miktoarm block copolymer/homopolymer blends of this study (filled symbols) and the linear diblock/homopolymer blends studies by Winey, Thomas, and Fetters[21] (open symbols).

Table 3. Table of Brush Heights and Swelling Ratios of the Blend Samples

	hPI (Å)	hPS (Å)	λ''	$\lambda^{\perp}_{\text{swollen phase}}$	$\lambda^{\perp}_{\text{unswollen phase}}$	*K*
I_2S-81	81.9	106.0	1.00	1.00	1.00	1.00
IY81−80	90.3	111.6	0.99	1.10	1.06	1.11
IY81−76	98.9	103.0	1.04	1.21	1.00	1.17
IY81−73	108.7	100.5	1.09	1.33	0.99	1.22
IY81−71	114.9	98.5	1.11	1.40	0.99	1.26
IY81−66	132.6	94.8	1.16	1.62	0.98	1.39
I_2S-81	81.9	106.0	1.00	1	1.00	1.00
SY81−82	81.3	153.4	1.00	1.03	0.99	1.03
SY81−85	71.9	155.4	1.07	1.05	0.88	0.98
I_2S-62	74.1	120.9	1.00	1.00	1.00	1.00
SY62−73	52.0	140.6	1.19	1.16	0.70	0.97
SY62−76	47.2	149.6	1.25	1.24	0.64	0.99
SY62−79	42.1	158.2	1.33	1.31	0.57	0.99

the effect of miktoarm star architecture plays a key role in the asymmetric swelling behavior. At the very least, the fact that there are two PI blocks per molecule in the PI block copolymer brush reduces the value of α for which swelling becomes homogeneous to something smaller than the value of 0.1 found for linear diblock containing blends. The IY81 series and the Winey 2600 g/mol hPS/linear diblock blend series have similar α values of 0.09 and 0.1, respectively. However, the IY81 series in which the homopolymer is blended into the two arm side of the block copolymer interface shows dramatic swelling anisotropy, while the linear diblock containing blend series shows isotropic behavior.

The miktoarm star molecular architecture of the block copolymer contributes to the differences in homopolymer swelling behavior on the two sides of the interface between the SY81 and SY62 series and in the IY81 series. The higher crowding of the grafted block copolymer brush on the PI side of the interface, due to the fact that there are two PI blocks per I_2S molecule,[11,47] may make it more difficult for the hPI to penetrate into the PI brush than for the hPS to penetrate the PS brush on the other side of the interface. In the IY81 series, this results in more hPI adding to the center of the PI domains rather than penetrating to the interface, thus increasing the domain thickness faster than the interfacial area as more homopolymer is added. On the other side of the interface, with one PS arm per block copolymer molecule, the hPS in the SY81 and SY62 series penetrates more easily into the brush resulting in more isotropic swelling behavior.

In diblock copolymer/low molecular weight homopolymer blends, the OOTs generally occur at the about the same overall volume fractions as those of pure diblock copolymer.[1−3] Additionally, an OOT occurs at the same volume fraction regardless of the direction from which it is approached, i.e., blending homopolymer A with a diblock that forms A cylinders in a B matrix to push it toward lamella, or blending B homopolymer with a lamellar diblock to push it back toward A cylinders.[1−3] In the present study, blending homopolymer into each sides of the interface in systems based on the asymmetric I_2S molecular architecture results in a splitting of the OOT location such that it occurs at different volume fractions depending on the direction from which it is approached. In the IY81 series, blending hPI with cylinder forming I_2S-81 results in a transition to lamella at $\phi_{PS} = 0.65$ to 0.66. This is a substantial shift from the cylinder to lamellar transition predicted by the Milner morphology diagram (around $\phi_{PS} \approx 0.80$), and is close to the PS volume fraction at the lamellar-cylinder OOT in linear diblocks. Figure 3 indicates that the OOTs of the SY62 series, in which a lamellar system is pushed toward cylinders by blending with hPS, occur at a ϕ_{PS} value closer to that predicted by the Milner theory for architecturally asymmetric I_2S molecules. The transition from lamella to perforated lamella occurs at a PS volume fraction between 0.79 and 0.82, and the transition from perforated lamella to cylinders occurs at a PS volume fraction between 0.82 and 0.85. In the IY81 blends series, neither perforated lamella nor Gyroid morphology was observed. The splitting of the OOTs in the SY62 and IY81 series most likely results from the asymmetry in the ability of the homopolymer to penetrate the PI and PS brushes due to the difference in chain crowding on the two sides of the interface in the I_2S material. The homopolymer must be able to effectively penetrate this brush in order to drive the changes in interfacial curvature which accompany an OOT.[1−3]

With the addition of increasing amounts of hPI in the IY89 series samples IY89−80 to IY89−71, the PI sheets forming the closed vesicles in IY89−82 become connected in a network of randomly ordered sheets that appear to form sample spanning structures, at least on the scale of our TEM observation. We speculate that the transition from a structure of predominantly closed vesicles and isolated sheets in IY89−82 to a structure

dominated by continuous sheets at higher hPI content may be a percolation phenomenon. During microphase separation of the sheetlike PI structure, there will be an energetic driving force to avoid free sheet edges. This can be accomplished by either forming closed vesicles or by producing a semi-infinite network of sheets. During the microphase separation process at lower overall PI content (IY89−82), embryonic pieces of microphase-separating sheet structure do not find enough neighboring sheet material to form a network and thus tend to close on themselves to produce vesicles. At slightly higher overall PI content, the percolation threshold is apparently reached and the microphase-separating sheets "find" enough like structure in the system to link up into a continuous network. Above the percolation threshold, there is no obvious morphology change from IY89−80 to IY89−71.

Conclusions

In blends of asymmetric I_2S block copolymer and homopolymers of either PS or PI, the order−order transitions were found to occur at different volume fractions depending on which type of homopolymer was used in the blends. Measurements of domain spacings showed that the PI homopolymer does not penetrate as well into the two-arm per molecule PI brush of the I_2S as does PS homopolymer into the one-arm per molecule PS brush on the PS side of the interface. This asymmetry of homopolymer brush penetration, brought about by the asymmetric architecture of the graft copolymer, leads to the splitting of the OOTs. Some of the blends produced interesting and unusual morphologies. For instance, sample SY62−82 formed well-ordered perforated lamella in which the perforated layers comprised only 18 vol % of the structure. This perforated lamellar morphology was found to be stable to thermal annealing. Unusual vesicle and continuous folded sheet morphologies were found in other blends. A transition between closed vesicles and continuous sheet structures was observed as a function of the overall concentration of the PI which forms the vesicle or sheet walls. This may result from percolation effects. When the PI concentration is lower, there is not enough material to form a continuous network of sheets, and isolated vesicles form instead. At higher PI concentrations, a percolation threshold is reached and the sheet structures can link up into a network.

Acknowledgment. Helpful discussions with D. J. Pochan and K. Laverdure are acknowledged. J.W.M and S.P.G acknowledge funding from the U.S Army Research Office (ARO) under Contracts DAAG55-98-1-0116 and DAAG55-98-1-0005. We acknowledge the use of instrumentation in the W. M. Keck Electron Microscopy Laboratory at the University of Massachusetts at Amherst, and Central Facility Support from Material Research Science and Engineering Center (MRSEC) at the University of Massachusetts at Amherst. The deuterated polystyrene was synthesized by Mr. David Uhrig of the University of Alabama at Birmingham.

References and Notes

(1) Winey, K. I.; Thomas, E. L.; Fetters, L. J. *Macromolecules* **1992**, *25*, 2645.
(2) Winey, K. I.; Thomas, E. L.; Fetters, L. J. *Macromolecules* **1992**, *25*, 422.
(3) Winey, K. I.; Thomas, E. L.; Fetters, L. J. *J. Chem. Phys.* **1991**, *95*, 9367.
(4) Pochan, D. J.; Gido, S. P.; Pispas, S.; Mays, J. W.; Ryan, A. J.; Fairclough, J. P. A.; Hamley, I. W.; Terrill, N. J. *Macromolecules* **1996**, *29*, 5091.
(5) Pochan, D. J.; Gido, S. P.; Pispas, S.; Mays, J. W. *Macromolecules* **1996**, *29*, 5099.
(6) Pochan, D. J.; Gido, S. P.; Zhou, J.; Mays, J. W.; Whitmore, M.; Ryan, A. J. *J. Polym. Sci., Polym. Phys.* **1997**, *35*, 2629.
(7) Lee, C.; Gido, S. P.; Poulos, Y.; Hadjichristidis, N.; Beck Tan, N.; Trevino, S. F.; Mays, J. W. *J. Chem. Phys.* **1997**, *107*, 6460.
(8) Lee, C.; Gido, S. P.; Poulos, Y.; Hadjichristidis, N.; Beck Tan, N.; Trevino, S. F.; Mays, J. W. *Polymer* **1997**, *39*, 4631.
(9) Lee, C.; Gido, S. P.; Pitsikalis, M.; Mays, J. W.; Beck Tan, N.; Trevino, S. F.; Hadjichristidis, N. *Macromolecules* **1997**, *30*, 3732.
(10) Gido, S. P.; Lee, C.; Pochan, D. J.; Pispas, S.; Mays, J. W.; Hadjichristidis, N. *Macromolecules* **1996**, *29*, 7022.
(11) Beyer, F. L.; Gido, S. P.; Poulos, Y.; Avgeropoulos, A.; Hadjichristidis, N. *Macromolecules* **1997**, *30*, 2373.
(12) Beyer, F. L.; Gido, S. P.; Veils, G.; Hadjichristidis, N.; Tan, N. B. *Macromolecules* **1999**, *32*, 6604.
(13) Milner, S. T. *Macromolecules* **1994**, *27*, 2333.
(14) Tselikas, Y.; Iatrou, H.; Hadjichristidis, N.; Liang, K. S.; Mohanty, K.; Lohse, D. J. *J. Chem. Phys.* **1996**, *105*, 2456.
(15) Matsushita, Y.; Noda, I. *Macromol. Symp.* **1996**, *106*, 251.
(16) Beyer, F. L.; Gido, S. P.; Uhrig, D.; Mays, J. W.; Tan, N. B.; Trevino, S. F. *J. Polym. Sci.* **1999**, *37*, 3392.
(17) Koizumi, S.; Hasegawa, H.; Hashimoto, T. *Macromolecules* **1994**, *27*, 6532.
(18) Hashimoto, T.; Tanaka, H.; Hasegawa, H. *Macromolecules* **1990**, *23*, 4378.
(19) Tanaka, H.; Hasegawa, H.; Hashimoto, T. *Macromolecules* **1991**, *24*, 240.
(20) Tanaka, H.; Hashimoto, T. *Macromolecules* **1991**, *24*, 5713.
(21) Winey, K. I.; Thomas, E. L.; Fetters, L. J. *Macromolecules* **1991**, *24*, 6128.
(22) Bates, F. S.; Maurer, W.; Lodge, T. P.; Schulz, M. F.; Matsen, M. W. *Phys. Rev. Lett.* **1995**, *75*, 4429.
(23) Disko, M. M.; Liang, K. S.; Behal, S. K.; Roe, R. J.; Jeon, K. J. *Macromolecules* **1993**, *26*, 2983.
(24) Norman, D. A.; Kane, L.; White, S. A.; Smith, S. D.; Spontak, R. J. *J. Mater. Sci. Lett.* **1998**, *17*, 545.
(25) Laurer, J. H.; Hajduk, D. A.; Dreckotter, S.; Smith, S. D.; Spontak, R. J. *Macromolecules* **1998**, *31*, 7546.
(26) Lesance, R. L.; Fetters, L. J.; Thomas, E. L. *Macromolecules* **1998**, *31*, 1680.
(27) Thomas, E. L.; Anderson, D. M.; Henkee, C. S.; Hoffman, D. *Nature* **1988**, *334*, 598.
(28) Khandpur, A. K.; Forster, S.; Bates, F. S. *Macromolecules* **1995**, *28*, 8796.
(29) Förster, S.; Khandpur, A. K.; Zhao, J.; Bates, F. S.; Hamley, I. W.; Ryan, A. J.; Bras, W. *Macromolecules* **1994**, *27*, 6922.
(30) Hajduk, D. A.; Harper, P. E.; Gruner, S. M.; Honeker, C. C.; Kim, G.; Thomas, E. L.; Fetters, L. J. *Macromolecules* **1994**, *27*, 4063.
(31) Vigilid, M. E.; Almdal, K.; Mortensen, K.; Hamley, I. W.; Fairclough, J. P. A.; Ryan, A. J. *Macromolecules* **1998**, *31*, 5702.
(32) Hajduk, D. A.; Ho, R.-M.; Hillimyer, M. A.; Bates, F. S.; Almdal, K. *J. Phys. Chem. B* **1998**, 1356.
(33) Hamley, I. W.; Gehlsen, M. D.; Khandpur, A. K.; Koppi, K. A.; Rosedale, J. H.; Schulz, M. F.; Bates, F. S.; Almdal, K.; Mortensen, K. *J. Phys. 2 France* **1994**, *4*, 2161.
(34) Burger, C.; Micha, M. A.; Oestereich, S.; S.Forster; Antonietti, M. *Europhys. Lett.* **1998**, *42*, 425.
(35) Ahn, J.-H.; Zin, W.-C. *Macromolecules* **2000**, *33*, 641.
(36) Hashimoto, T.; Koizumi, S.; Hasegawa, H.; Izumitani, T.; Hyde, S. T. *Macromolecules* **1992**, *25*, 1443.
(37) Semenov, A. N. *Sov. Phys. JETP* **1985**, *61*, 733.
(38) Fredrickson, G. H. *Macromolecules* **1991**, *24*, 3456.
(39) Qi, S.; Wang, Z.-G. *Phys. Rev. Lett.* **1996**, *76*, 1679.
(40) Qi, S.; Wang, Z.-G. *Phys. Rev. E* **1997**, *55*, 1682.
(41) Qi, S.; Wang, Z.-G. *Macromolecules* **1997**, *30*, 4491.
(42) Shull, K. R.; Winey, K. I. *Macromolecules* **1992**, *25*, 2637.
(43) Laverdure, K.; Gido, S. P.; Pispas, S.; Mays, J. W. Manuscript in preparation.
(44) Oster, G.; Riley, D. P. *Acta Crystyllogr.* **1952**, *5*, 272.
(45) Oster, G.; Riley, D. P. *Acta Crystallogr.* **1952**, *5*, 1.
(46) Matsen, M. W. *Macromolecules* **1995**, *28*, 5765.
(47) Zhu, Y.; Gido, S. P. Manuscript in preparation.
(48) Bates, F. S.; Berney, C. V.; Cohen, R. E. *Macromolecules* **1983**, *16*, 1101.

MA001901V